Chemical bonding and many-body effects in site-specific x-ray photoelectron spectra of corundum V_2O_3

J. C. Woicik,[1] M. Yekutiel,[2] E. J. Nelson,[1] N. Jacobson,[2] P. Pfalzer,[3] M. Klemm,[3] S. Horn,[3] and L. Kronik[2,*]
[1]*National Institute of Standards and Technology, Gaithersburg, Maryland 20899, USA*
[2]*Department of Materials and Interfaces, Weizmann Institute of Science, Rehovoth 76100, Israel*
[3]*Institut für Physik, Universtitätsstrasse 1, 86159 Augsburg, Germany*
(Received 24 January 2007; revised manuscript received 24 July 2007; published 1 October 2007)

Site-specific x-ray photoelectron spectroscopy together with density functional theory calculations based on the local density approximation have identified the chemical bonding, single-particle matrix element, and many-body effects in the x-ray photoelectron spectrum of corundum V_2O_3. Significant covalent bonding in both the upper and lower lobes of the photoelectron spectrum is found, despite the localized nature of the V 3*d* electrons that are responsible for the Mott behavior. We show that the approximate treatment of correlation dominates the discrepancy between theory and experiment in the near-Fermi-edge region and that many-body effects of the photoemission process can be modeled by Doniach-Šunjić [J. Phys. C **3**, 285 (1970)] asymmetric loss. Correlation effects govern the relative intensity and energy position of the higher level electron bands, and many-body effects dominate the "tail" region of both the upper and lower lobes of the photoemission spectrum.

DOI: 10.1103/PhysRevB.76.165101 PACS number(s): 79.60.−i, 71.30.+h, 78.70.Ck

I. INTRODUCTION

Vanadium sesquioxide, V_2O_3, is a highly correlated solid that has been studied intensively for over three decades. At room temperature, V_2O_3 is a paramagnetic metal possessing a trigonal (corundum) crystal structure. Upon cooling to ≈160 K, it undergoes a first order phase transition to an insulating antiferromagnet with monoclinic symmetry.[1] This transition is often considered a prototypical Mott-Hubbard metal-insulator transition.[2,3] However, more recent work suggests a more refined model to account for covalent bonding between the V 3*d* and O 2*p* states.[4,5]

Photoelectron spectroscopy (PES) of the paramagnetic V_2O_3 phase has been used intensively in an attempt to understand the underlying electronic structure in general, hybridization trends in particular, and their relation to the metal-insulator transition.[5–13] Unfortunately, interpretation of the PES data is not straightforward. Ultraviolet photoelectron spectroscopy (UPS) is highly surface sensitive, and its results may deviate from the bulk electronic structure. X-ray photoelectron spectroscopy (XPS) is more sensitive to the true bulk electronic structure owing to the larger escape depth of the photoelectrons. Indeed, recent high-resolution XPS studies[12,13] have detected a prominent near-Fermi-level peak that was not revealed by earlier UPS investigations.[6,8,11] However, the interpretation of XPS data is, in general, also complicated. First, matrix element effects; i.e., the modulation of the photoelectron spectrum by the transition probabilities between the initial, bound-state valence electrons and the final, plane-wave continuum-state photoelectrons, are pronounced in XPS.[14] Second, the analysis of XPS data is more complicated than suggested by a single-particle description due to many-electron effects in the photoemission process.[14,15]

In this paper, we employ site-specific XPS (SSXPS),[16] where XPS data are collected under conditions of x-ray Bragg diffraction, for a *direct* experimental determination of the contribution of the V and O atoms to the overall electronic structure of V_2O_3 in its metallic paramagnetic phase. By contrasting these measurements with first principles calculations based on density functional theory (DFT) within the local density approximation (LDA),[17] we quantify the extent to which matrix element effects dominate the photoelectron spectra. By comparing the SSXPS results with additional high-resolution near-Fermi-edge XPS measurements as well as core-level ones, we identify the signature of many-body effects in the photoemission process and show the importance of both Doniach-Šunjić[18] electron shakeup across the Fermi edge and the approximate treatment of correlation in LDA in determining the relative intensity and energy position of the upper electron bands.

II. EXPERIMENTAL AND COMPUTATIONAL DETAILS

The experiment was performed at the National Synchrotron Light Source, Brookhaven National Laboratory, at the National Institute of Standards and Technology tender x-ray spectroscopy facility beamline X24A. A double crystal monochromator was operated with Si(111) crystals and high-resolution photoelectron spectra were obtained with a hemispherical electron analyzer. An atomically clean, stoichiometric single-crystal corundum $V_2O_3(0001)$ surface was prepared by annealing to ≈725 °C in ultrahigh vacuum after which low-energy electron diffraction showed a sharp 1×1 pattern. Photoelectron spectra were recorded at two different photon energies within the photon-energy width ($\Delta E \approx 0.6$ eV) of the corundum $V_2O_3(10\bar{1}4)$ Bragg backreflection condition ($h\nu \approx 2286$ eV); they were recorded with the photon beam incident to the (0001) surface at ≈51°. Photon energies were chosen to maximize the electric-field intensity on either the V or the O atomic planes. Partial V and O valence spectra were then computed by taking linear combinations of the spectra recorded within the width of the V_2O_3 crystal x-ray rocking curve. Valence spectra were also recorded at photon energy ≈5 eV below the Bragg condi-

tion, and higher-energy resolution near-Fermi-level and core-level spectra were recorded as well. Additional details on the SSXPS technique are given in the literature.[16]

Density functional theory calculations for the total and partial density of states were performed using the PARATEC code[19] by employing *ab initio* Troullier-Martins pseudopotentials[20] within the local density approximation,[21] with a plane-wave basis. Pseudopotentials based on electronic configurations of $3s^2 3p^6 4s^0 3d^3$ (V) and $2s^2 2p^4$ (O) were used, with $s/p/d$ (V) and s/p (O) cutoff radii (in a.u.) of 1.54/1.54/2.5 and 1.34/1.45, respectively. A plane-wave cutoff energy of 140 Ry and a $4\times4\times4$ Monkhorst-Pack k-point sampling scheme[22] were used to guarantee convergence. All calculations were performed at the experimental corundum geometry of $a=5.647$ Å, $u(\mathrm{V})=0.3463$, and $u(\mathrm{O})=0.565$.[23] The ensuing density of states was in excellent agreement with previous LDA calculations,[24] obtained using a different method (the linearized augmented plane-wave technique), confirming the adequacy of the above-given parameters.

III. CHEMICAL HYBRIDIZATION AND MATRIX ELEMENT EFFECTS

Partial V and O photoelectron spectra of the V_2O_3 valence electronic structure, obtained using SSXPS, are shown in Figs. 1(a) and 1(b), respectively. The total (usual) off-Bragg XPS valence-electron spectrum is given in Fig. 1(c). In Fig. 1, each experimental spectrum is compared with several theoretical spectra, each representing the filled-state portion of the density of states (DOS) curve, as obtained from the LDA calculation, convolved with a Gaussian of width 0.47 eV to mimic the total experimental resolution. The curves denoted by "DOS" and "p-DOS" are simply the total and partial theoretical valence DOS, respectively [partial in Figs. 1(a) and 1(b), and total in Fig. 1(c)]. Also shown in Figs. 1(a) and 1(b) are the theoretical *per-orbital* partial valence DOS curves of V 3*d*, V 4*s*, and V 4*p* and O 2*s*, and O 2*p*, respectively. The curves denoted by "c-DOS" and "cc-DOS" are explained below.

Both theoretical and experimental spectra in Fig. 1 feature two "lobes" — a lower intensity, narrower lobe extending from the Fermi level to ≈−3 eV (denoted below as the "upper lobe") and a higher intensity, wider lobe extending from ≈−3 to ≈−9 eV (denoted below as the "lower lobe"). The per-orbital partial DOS curves show a dominating contribution from the V 3*d* and O 2*p* orbitals to the upper and lower lobes, respectively, which agrees with the usual assignment of these features to V 3*d* and O 2*p* electron bands.[12] Simple electron counting assuming a formal 3^+ charge on the V ion shows that each V atom is "left" with two valence electrons beyond what is necessary for bonding the O atoms. These electrons make up most of the contribution to the high-kinetic-energy upper lobe and are, of course, related to the metallic property of the phase.

Importantly, the partial XPS data of Figs. 1(a) and 1(b) show that both V and O electrons contribute non-negligibly to the overall electronic structure at all probed energies. Furthermore, all spectral features of both the experimental and theoretical V and O partial curves occur at exactly the same energy. This is an immediate consequence of the sharing of electrons in a covalent bond; i.e., electrons shared between the V and O atoms have a finite probability of being photoemitted from either. Interestingly, the complete hybridization of features between the partial DOS of the V metal atoms and of the O ligand atoms has been observed previously in SSXPS of α-Fe_2O_3.[25] However, in SSXPS of TiO_2,[26] the O partial DOS features a *triply* peaked structure, where the third, upper peak has no counterpart in the Ti partial DOS spectrum, revealing the nonbonding and insulating character of these O states in the electronic structure of TiO_2.

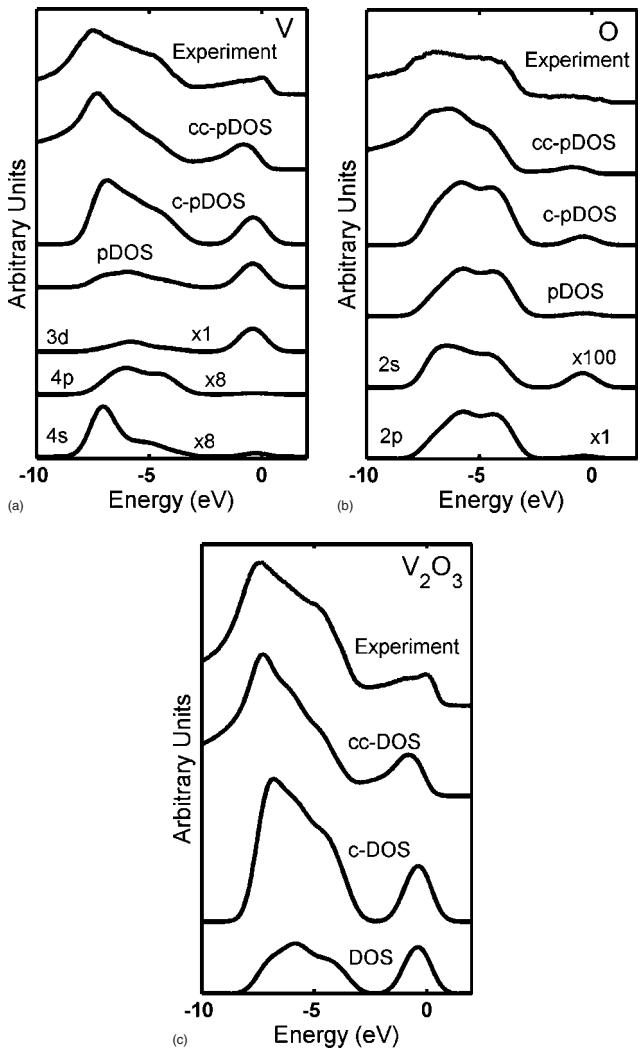

FIG. 1. Experimental valence-photoelectron spectra ($h\nu\approx2286$ eV), theoretical density of states curves (DOS), theoretical density of states curves corrected for individual angular-momentum dependent photoelectron cross sections (c-DOS), and theoretical density of states curves corrected for both individual angular-momentum dependent photoelectron cross sections and the Doniach-Šunjić effect (cc-DOS) for (a) V, (b) O, and (c) total spectrum. p indicates partial DOS. (a) and (b) additionally show partial angular-momentum-resolved DOS curves for V 3*d*, V 4*s*, and V 4*p*, and O 2*s* and O 2*p*, respectively. Curves have been scaled to equal peak heights.

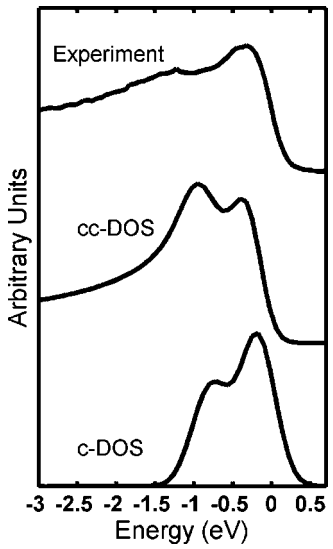

FIG. 2. High-resolution photoelectron spectrum of the near-Fermi region ($h\nu \approx 2286$ eV), compared to the theoretical density of states in that region. Experimental valence-photoelectron spectrum (top), theoretical density of states curve corrected for individual angular-momentum dependent photoelectron cross sections (c-DOS) (bottom), and theoretical density of states curve corrected for both individual angular-momentum dependent photoelectron cross sections and the Doniach-Šunjić effect (cc-DOS) (middle). Curves have been scaled to equal peak heights.

Indirect evidence of V $3d$-O $2p$ hybridization has been given before, either by resonant photoemission measurements[7,9] or by comparison of photoemission data to theory.[4,5] Here, the covalent bonding is directly measured by the V and O contributions to the photoelectron spectrum. This direct observation of p-d hybridization demonstrates that the traditional view of V_2O_3 as a pure Mott-Hubbard material is too simplistic and supports more modern theories that explicitly account for hybridization between the metal and ligand.[4,5,27]

Because the photoexcitation process conserves angular momentum, in a single-particle approximation the valence photocurrent may be written as[14]

$$I(E,h\nu) \propto \sum_{i,j} \rho_{i,j}(E)\sigma_{i,j}(E,h\nu). \quad (1)$$

Here $\rho_{i,j}(E)$ are the individual, angular-momentum j resolved, partial DOS of the individual i atoms of the crystalline unit cell, and the $\sigma_{i,j}(E,h\nu)$ are the angle-integrated, angular-momentum dependent, photoionization cross sections.

As seen from Figs. 1 and 2, using Eq. (1) to compute the V and O partial photoelectron curves as the *weighted sum* of the different orbital components (curves denoted by "c-pDOS" and "c-DOS" are the cross-section *corrected* partial and total theoretical DOS curves, respectively) improves agreement with experiment. We used weighting coefficients that were empirically found to best mimic the experimental spectra: $(\mathrm{O}\ 2s)/(\mathrm{O}\ 2p)=7.3$ and $(\mathrm{V}\ 4s)/(\mathrm{V}\ 3d)=40.4$. As demonstrated previously for TiO_2,[26] these weighting coefficients are within a factor of 2 of the theoretical *atomic* photoemission cross sections.[28]

For the V partial DOS curve shown in Fig. 1(a), improvement is in both the line shape of the lower lobe and in the relative intensity between the upper and lower lobes. This is because the experimental V spectrum is dominated by V $4s$ (and $4p$) electrons due to their higher atomic cross sections, while the uncorrected theoretical V partial DOS is dominated by V $3d$ electrons. However, for the O partial DOS curve shown in Fig. 1(b), although noticeable, improvement in the agreement between theory and experiment is not as significant. Clearly then, the discrepancy between theory and experiment for the O spectrum is not due to matrix element effects. This is because the contribution of O $2s$ electrons is relatively small even when their enhanced cross section is taken into account.

IV. MANY-BODY EFFECTS

While the matrix-element-corrected LDA calculation describes the lower lobe of the photoemission spectrum, Figs. 1(a)–1(c) show that it fails to predict the line shape of the upper lobe. The difference is more easily observed in a higher-resolution XPS spectrum of the near-Fermi-edge region, shown in Fig. 2. Also shown in the figure is the matrix-element-corrected c-DOS curve broadened by 0.2 eV.

Both experiment and c-DOS calculation feature two peaks: one near the Fermi edge and one at energies lower by over an eV. A group-theoretical analysis of the LDA peaks shows that they correspond to a splitting of the V $3d$-derived t_{2g} states into a_{1g} (lower peak) and e_g^{π} (upper peak) states.[29] This splitting results from distortion of the octahedral geometry surrounding the V atoms within the D_{3d} point group; similar analysis has been successful for tetragonally distorted $SrTiO_3$ in C_{4v} symmetry.[30] Clearly, the c-DOS curve predicts neither the energy separation between the two peaks nor their relative intensity. Furthermore, a significant low-energy "tail," extending for over an eV, is observed in the experimental spectrum. This tail has no counterpart in the theoretical LDA curve.

The limitations of LDA calculations in describing the experimental XPS data can be attributed to two different physical sources, the first being the treatment of electron correlation. Within LDA, one assumes that at each point in space the exchange-correlation energy per particle is given by its value for the homogeneous electron gas.[17] While this approximation is sufficient for many simple metals and semiconductors, it is too crude to describe a highly correlated material correctly, and, in fact, LDA fails to predict the metal-insulator transition in V_2O_3. The LDA results presented here (and elsewhere, e.g., in Refs. 5, 10, 24, and 29) are compared to the room temperature metallic phase, even though the 0 K electronic structure is computed. This approximate treatment of correlation can also lead to an inaccurate distribution of excitation energies. In many correlated materials agreement with experiment is improved by adding an on-site Hubbard Coulomb interaction term U for the localized d (or f) electrons.[31] However, we are not aware of LDA+U calculations for the metallic, paramagnetic V_2O_3

phase, and whether or not LDA+U would provide an adequate description for V_2O_3 is controversial.[32]

The second source of error within DFT is the use of the Kohn-Sham eigenvalues. These solutions are only zero-order approximations of quasiparticle excitation energies.[33] Many-electron processes of photoexcitation attributed to screening and relaxation of the valence hole beyond the quasiparticle approximation therefore will not be contained within a DFT calculation. Multiple configurations in the photoemission final state can be considered explicitly by *ad hoc* calculations within a cluster solution of a model Hamiltonian using a configuration-interaction expansion. An empirical solution to this problem has recently rendered good agreement with experiment.[4,5]

An alternative approach to the problem of strong electron correlation is dynamical mean field theory (DMFT).[34] In this approximation, the many-body spectral response function (that results from excitation of the many-electron wave function) near the Fermi energy is computed by mapping the Hubbard model onto a self-consistent quantum impurity model. Agreement with the near-Fermi-level XPS data is found, given a reasonable choice for the many-body Coulomb repulsion parameter U,[12,13,34] and, in fact, by fitting U, the metal insulator transition not predicted by *ab initio* LDA calculations is recovered.

In order to distinguish the effects of approximate correlation in the LDA calculation from the effects of intrinsic many-body phenomena in the photoemission process, we modeled the latter by the Doniach-Šunjić asymmetric line shape due to electron shakeup across the Fermi edge.[18] These effects are present even in the simple metals that are well described by LDA. Further motivation is provided by Fig. 3(a), which compares the XPS spectrum of the V $2p_{3/2}$ core level with the XPS spectrum of the V_2O_3 valence band, and by Fig. 3(b), which compares the XPS spectrum of the Ti $2p_{3/2}$ core level and the XPS spectrum of the TiO_2 valence band.[26] Tailing appears in both valence and core spectra for V_2O_3, but not in valence and core spectra for TiO_2, suggesting a common physical origin associated with the metallicity of V_2O_3 and the absence of a Fermi edge for insulating TiO_2. Additionally, there appears to be a distinct correlation between the presence of a valence-band tail and the appearance of both similar and more complicated features in the core-level spectrum of V_2O_3. Similar tails in the core-level spectra of V_2O_3 have been observed previously[35,36] and have been interpreted as such. This assertion also agrees with the recent data of Ref. 13 where a clear correlation between the shake-down satellites in the V $2p$ and $3p$ core-level spectra and the spectral peak measured at the Fermi level was observed.

We have incorporated the Doniach-Šunjić effect by convolving the theoretical LDA calculations with the asymmetric power-law Doniach-Šunjić line shape, $E^{\alpha-1}$. This procedure neglects, among other things, a dependence of α on the energy and the contribution of additional lifetime effects. A physically reasonable[18] value of $\alpha=0.25$ was determined from a fit to the O $1s$ spectrum of V_2O_3. Figures 1 and 2 show the calculations *corrected* for the Doniach-Šunjić effect denoted by "cc." In all cases, agreement with experiment is markedly improved. In particular, the tail region, which was completely missed by the DOS and c-DOS curves, is well

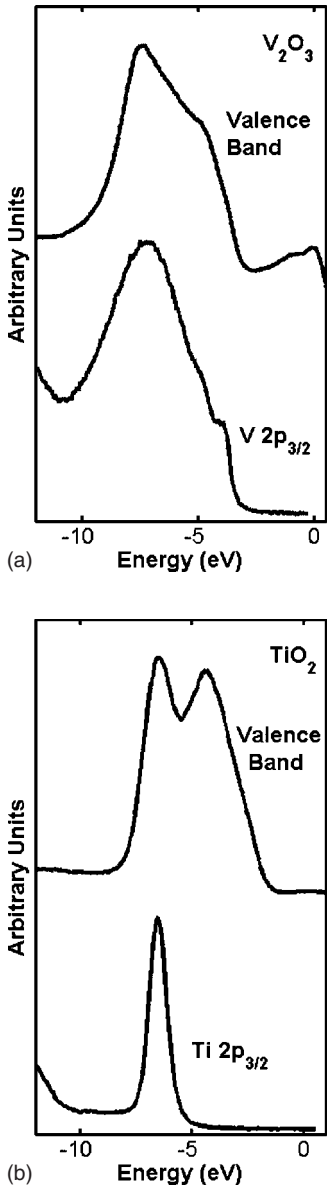

FIG. 3. Comparison of the $2p_{3/2}$ core level and the valence-band photoemission spectra for (a) V_2O_3 ($h\nu\approx2286$ eV) and (b) TiO_2 ($h\nu\approx2695$ eV). Curves have been scaled to equal peak heights and shifted in binding energy.

reproduced by the cc-DOS curve, not only for the upper lobe, but also for the lower lobe. However, the relative intensity and energy position of the two peaks of the near-Fermi region is still lacking.

Based on this analysis, we conclude that the features corresponding to the two highest electron bands, which are not fully described even after the correction for asymmetric line shape, are sensitive to the many-body correlations not properly accounted for within LDA. In fact, the presence of the higher-energy peak (and energy position of the lower peak) is dependent on whether or not V_2O_3 is in its insulating or metallic phase,[12] which is mimicked by choice of energy parameter U within DMFT. Within LDA, this peak is due to a cutoff of the density of states from a partially filled metallic band by the Fermi edge. Within DMFT, it is described by the

coherent part of the spectral function similarly cut off by the Fermi edge.

V. CONCLUSIONS

We have used site-specific x-ray photoelectron spectroscopy to measure the chemical bonding, matrix element, and many-body effects in the x-ray photoelectron spectra of corundum V_2O_3. We have identified significant covalent bonding in both the upper and lower lobes of the photoemission data, despite the localized nature of the V 3*d* electrons that are responsible for the Mott behavior. Furthermore, we have shown that much of the disagreement between theoretical LDA calculations and experimental spectra are due to single-particle matrix element effects and many-body asymmetric loss features intrinsic to the photoemission process. Lack of adequate correlation in LDA affects most significantly the relative intensity and energy separation of the two electron bands near the Fermi level.

ACKNOWLEDGMENTS

We thank Ehud Altman (Weizmann Institute), Yuval Gefen (Weizmann Institute), Steven Louie (UC Berkeley), and Jim Chelikowsky (University of Texas) for illuminating discussions. This work was supported by a US-Israel Bi-National Science Foundation Grant and was made possible in part by the historic generosity of the Harold Perlman family. Use of the National Synchrotron Light Source, Brookhaven National Laboratory, was supported by the U.S. Department of Energy, Office of Science, Office of Basic Energy Sciences, under Contract No. DE-AC02-98CH10886. Additional support was provided by the Deutsche Forschungsgemeinschaft (DFG) through Sonderforschungsbereich (SFB) 484. E.J.N. thanks the National Research Council for support.

*leeor.kronik@weizmann.ac.il

[1] P. D. Dernier and M. Marezio, Phys. Rev. B **2**, 3771 (1970).
[2] D. B. McWhan, T. M. Rice, and J. P. Remeika, Phys. Rev. Lett. **23**, 1384 (1969).
[3] J. Zaanen, G. A. Sawatzky, and J. W. Allen, Phys. Rev. Lett. **55**, 418 (1985).
[4] R. J. O. Mossanek and M. Abbate, Phys. Rev. B **75**, 115110 (2007).
[5] R. Zimmermann, R. Claessen, F. Reinert, P. Steiner, and S. Hüfner, J. Phys.: Condens. Matter **10**, 5697 (1998); R. Zimmermann, P. Steiner, R. Claessen, F. Reinert, S. Hüfner, P. Blaha, and P. Dufek, *ibid.* **11**, 1657 (1999).
[6] G. A. Sawatzky and D. Post, Phys. Rev. B **20**, 1546 (1979).
[7] K. E. Smith and V. E. Henrich, Phys. Rev. B **38**, 5965 (1988); **38**, 9571 (1988).
[8] S. Shin, S. Suga, M. Taniguchi, M. Fujisawa, H. Kanzaki, A. Fujimori, H. Daimon, Y. Ueda, K. Kosuge, and S. Kachi, Phys. Rev. B **41**, 4993 (1990).
[9] M. Imada, A. Fujimori, and Y. Tokura, Rev. Mod. Phys. **70**, 1039 (1998).
[10] H. D. Kim, H. Kumigashira, A. Ashihara, T. Takahashi, and Y. Ueda, Phys. Rev. B **57**, 1316 (1998).
[11] M. Schramme, Ph. D. thesis, Universität Augsburg, 2000; some of Schramme's experimental results are shown in K. Held, G. Keller, V. Eyert, D. Vollhardt, and V. I. Anisimov, Phys. Rev. Lett. **86**, 5345 (2001).
[12] S. K. Mo, J. D. Denlinger, H. D. Kim, J. H. Park, J. W. Allen, A. Sekiyama, A. Yamasaki, K. Kadono, S. Suga, Y. Saitoh, T. Muro, P. Metcalf, G. Keller, K. Held, V. Eyert, V. I. Anisimov, and D. Vollhardt, Phys. Rev. Lett. **90**, 186403 (2003).
[13] G. Panaccione, M. Altarelli, A. Fondacaro, A. Georges, S. Huotari, P. Lacovig, A. Lichtenstein, P. Metcalf, G. Monaco, F. Offi, L. Paolasini, A. Poteryaev, M. Sacchi, and O. Tjernberg, Phys. Rev. Lett. **97**, 116401 (2006).
[14] S. Hüfner, *Photoelectron Spectroscopy: Principles and Applications*, 2nd ed. (Springer, Berlin, 1996).
[15] P. A. Cox, *Transition Metal Oxides* (Clarendon, Oxford, 1992).
[16] J. C. Woicik, E. J. Nelson, and P. Pianetta, Phys. Rev. Lett. **84**, 773 (2000); J. C. Woicik, E. J. Nelson, T. Kendelewicz, P. Pianetta, M. Jain, L. Kronik, and J. R. Chelikowsky, Phys. Rev. B **63**, 041403(R) (2001); J. C. Woicik, E. J. Nelson, D. Heskett, J. Warner, L. E. Berman, B. A. Karlin, I. A. Vartanyants, M. Z. Hasan, T. Kendelewicz, Z. X. Shen, and P. Pianetta, *ibid.* **64**, 125115 (2001).
[17] D. M. Ceperley and B. J. Alder, Phys. Rev. Lett. **45**, 566 (1980); J. P. Perdew and Y. Wang, Phys. Rev. B **45**, 13244 (1992).
[18] S. Doniach and M. Šunjić, J. Phys. C **3**, 285 (1970).
[19] www.nersc.gov/projects/paratec; see also J. Ihm, A. Zunger, and M. L. Cohen, J. Phys. C **12**, 4409 (1979).
[20] N. Troullier and J. L. Martins, Phys. Rev. B **43**, 1993 (1991).
[21] D. M. Ceperley and B. J. Alder, Phys. Rev. Lett. **45**, 566 (1980); J. P. Perdew and Y. Wang, Phys. Rev. B **45**, 13244 (1992).
[22] H. J. Monkhorst and J. D. Pack, Phys. Rev. B **13**, 5188 (1976).
[23] R. W. G. Wyckoff, *Crystal Structures* (Interscience, New York, 1967), Vol. 2, pp. 7–8.
[24] L. F. Mattheiss, J. Phys.: Condens. Matter **6**, 6471 (1994).
[25] C. Y. Kim, M. J. Bedzyk, E. J. Nelson, J. C. Woicik, and L. E. Berman, Phys. Rev. B **66**, 085115 (2002).
[26] J. C. Woicik, E. J. Nelson, L. Kronik, M. Jain, J. R. Chelikowsky, D. Heskett, L. E. Berman, and G. S. Herman, Phys. Rev. Lett. **89**, 077401 (2002).
[27] I. Pollini, J. Electron Spectrosc. Relat. Phenom. **152**, 107 (2006).
[28] M. B. Trzhaskovskaya, V. I. Nefedov, and V. G. Yarzhemsky, At. Data Nucl. Data Tables **77**, 97 (2001); as the V 4*p* orbitals are unoccupied in the free V atom, the V 4*p* atomic cross section is not tabulated; consequently, we took it to be equal to the V 4*s* one.
[29] V. Eyert, U. Schwingenschlögl, and U. Eckern, Europhys. Lett. **70**, 782 (2005).
[30] J. C. Woicik, E. L. Shirley, C. S. Hellberg, K. E. Anderson, S. Sambasivan, D. A. Fischer, B. D. Chapman, E. A. Stern, P. Ryan, D. L. Ederer, and H. Li, Phys. Rev. B **75**, 140103(R) (2007).
[31] V. I. Anisimov, F. Aryasetiawan, and A. I. Lichtenstein, J. Phys.:

Condens. Matter **9**, 767 (1997).
[32] S. Di Matteo, Phys. Scr. **71**, CC1 (2005), and references therein.
[33] A. Görling, Phys. Rev. A **54**, 3912 (1996); C. Filippi, C. J. Umrigar, and X. Gonze, J. Chem. Phys. **107**, 9994 (1997).
[34] G. Kotliar, S. Y. Savrasov, K. Haule, V. S. Oudovenko, O. Parcollet, and C. A. Marianetti, Rev. Mod. Phys. **78**, 865 (2006); G. Kotliar and D. Vollhardt, Phys. Today **57**(3), 53 (2004). K. Held, I. A. Nekrasov, G. Keller, V. Eyert, N. Blümer, A. K. McMahan, R. T. Scalettar, Th. Pruschke, V. I. Anisimov, and D. Vollhardt, Psi-k Newsletter **56**, 65 (2003); http://psi-k.dl.ac.uk/newsletters/news_56/highlight_56.pdf.
[35] R. L. Kurtz and V. E. Henrich, Phys. Rev. B **28**, 6699 (1983).
[36] K. E. Smith and V. E. Henrich, Phys. Rev. B **50**, 1382 (1994).